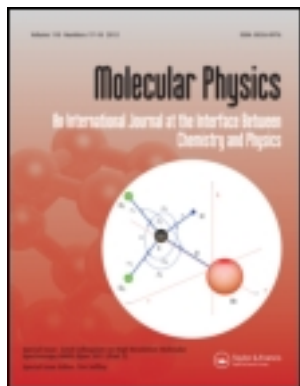


This article was downloaded by: [Michigan State University]

On: 27 November 2013, At: 00:50

Publisher: Taylor & Francis

Informa Ltd Registered in England and Wales Registered Number: 1072954 Registered office: Mortimer House, 37-41 Mortimer Street, London W1T 3JH, UK



## Molecular Physics: An International Journal at the Interface Between Chemistry and Physics

Publication details, including instructions for authors and subscription information:

<http://www.tandfonline.com/loi/tmph20>

### Energetics of graphene flakes

Zacharias G. Fthenakis<sup>ab</sup>

<sup>a</sup> Department of Physics and Astronomy, Michigan State University, East Lansing, MI, USA

<sup>b</sup> Institute of Electronic Structure and Laser, Foundation of Research and Technology, Heraklion - Crete, Greece

Accepted author version posted online: 06 Mar 2013. Published online: 28 Mar 2013.

To cite this article: Zacharias G. Fthenakis (2013) Energetics of graphene flakes, *Molecular Physics: An International Journal at the Interface Between Chemistry and Physics*, 111:21, 3289-3296, DOI: [10.1080/00268976.2013.782437](https://doi.org/10.1080/00268976.2013.782437)

To link to this article: <http://dx.doi.org/10.1080/00268976.2013.782437>

PLEASE SCROLL DOWN FOR ARTICLE

Taylor & Francis makes every effort to ensure the accuracy of all the information (the "Content") contained in the publications on our platform. However, Taylor & Francis, our agents, and our licensors make no representations or warranties whatsoever as to the accuracy, completeness, or suitability for any purpose of the Content. Any opinions and views expressed in this publication are the opinions and views of the authors, and are not the views of or endorsed by Taylor & Francis. The accuracy of the Content should not be relied upon and should be independently verified with primary sources of information. Taylor and Francis shall not be liable for any losses, actions, claims, proceedings, demands, costs, expenses, damages, and other liabilities whatsoever or howsoever caused arising directly or indirectly in connection with, in relation to or arising out of the use of the Content.

This article may be used for research, teaching, and private study purposes. Any substantial or systematic reproduction, redistribution, reselling, loan, sub-licensing, systematic supply, or distribution in any form to anyone is expressly forbidden. Terms & Conditions of access and use can be found at <http://www.tandfonline.com/page/terms-and-conditions>

## RESEARCH ARTICLE

### Energetics of graphene flakes

Zacharias G. Fthenakis<sup>a,b,\*</sup>

<sup>a</sup>Department of Physics and Astronomy, Michigan State University, East Lansing, MI, USA; <sup>b</sup>Institute of Electronic Structure and Laser, Foundation of Research and Technology, Heraklion - Crete, Greece

(Received 23 January 2013; final version received 28 February 2013)

Based on the idea that the binding energy of a graphene flake is a sum of atomic energy contributions, which depend on the local atomic environment of each atom of the flake, we propose a model for graphene flake energetics, which can very accurately predict the cohesive energy  $U_{\text{coh}}$  of graphene flakes. In our study, we calculate the cohesive energy of hexagonal graphene flakes with up to  $\approx 1000$  atoms using the tight binding molecular dynamics method and we show that the calculated  $U_{\text{coh}}$  values fit extremely accurately to the  $U_{\text{coh}}$  expression derived from the proposed model. For a further validation, we show that the proposed  $U_{\text{coh}}$  expression can very accurately predict the calculated  $U_{\text{coh}}$  values of other graphene flakes with random shapes. Based on that model, we show that the graphene flake stability obeys the following rules: (1) Between isomers the most stable are those with the larger number of bonds (or equivalently, with the smaller number of edge atoms) and (2) between isomers with the same number of bonds (or with the same number of edge atoms), the most stable are those with the smaller number of zig-zag atoms.

**Keywords:** graphene flakes; energetics; cohesive energy; stability rules; model; tight binding molecular dynamics

#### 1. Introduction

After the isolation of monolayer graphene sheets [1], it was obvious that the study of the properties of graphene flakes would follow. Graphene flakes have been experimentally produced [2–8], and many of their properties have been studied both theoretically [9–26] and experimentally [3,4,27]. However, only some few computational studies [9–11] have been dedicated to the graphene flake energetics, up to date. Among those studies, Barnard and Snook [9] used density-functional tight binding simulations to study the energy dependence of hexagonal graphene flakes with un-terminated, monohydride and dihydride edges. From their energy plots, one can see that the cohesive energy  $U_{\text{coh}}$  (i.e. binding energy per atom) decreases monotonically versus the number of atoms  $N$ . Nakajima and Shintani [10] used classic potential molecular dynamics simulations to calculate the energy of graphene disks and hexagonal flakes with up to 5000 atoms. The figures they presented show a monotonic decrease of  $U_{\text{coh}}$  as a function of the flake diameter. Kuc *et al.* [11] used the density functional-based tight binding method to calculate the energy of graphene flake isomers of various topologies, with up to 220 atoms. From their study, they concluded that among those isomers the most stable are the circular flakes, while the least stable are the very narrow ones. Based on the consideration that the cohesive energy  $U_{\text{coh}}$  of the flakes should depend on the edge-to-surface ratio, they concluded that the cohesive

energy of a graphene flake should be written as

$$U_{\text{coh}} = \varepsilon_{\infty} + c \frac{N_s}{N} \quad (1)$$

or

$$U_{\text{coh}} = \varepsilon_{\infty} + \frac{c'}{\sqrt{N}}, \quad (2)$$

where  $\varepsilon_{\infty}$  is the cohesive energy of graphene,  $N_s$  is the number of edge atoms and  $c$ ,  $c'$  are adjustable constants. However, plotting  $U_{\text{coh}}$  against  $1/\sqrt{N}$  they found that the overall behaviour of  $U_{\text{coh}}$  against  $1/\sqrt{N}$  is far from linear, but there is a much better linear correlation between  $U_{\text{coh}}$  and  $N_s/N$ .

With the present study, we improve the above-mentioned works. We introduce a new model, based on the assumption that the energy of a cluster depends on the local atomic environment of the cluster atoms. Similar approach has been proposed by Tománek *et al.* [28], for the estimation of the cohesive energy of transition metal clusters. Based on the proposed model we present an expression for  $U_{\text{coh}}$ , which can very accurately predict the cohesive energy of any graphene flake.

To show the validity of the proposed model, we first calculate the cohesive energy values of the hexagonal graphene flakes with up to  $\approx 1000$  atoms, using the tight binding

\*Corresponding author. Email: [fthenak@msu.edu](mailto:fthenak@msu.edu)

molecular dynamics method [29–31]. Then using some reasonable assumptions for the local atomic environment of the flake atoms and gradually improving them, we derive general expressions for the cohesive energy of graphene flakes, with increasing accuracy. Using those expressions, we derive expressions especially for hexagonal graphene flakes with zig-zag edges (HGF-ZZ). Fitting the calculated  $U_{\text{coh}}$  values of HGF-ZZ to those expressions, we test their ability to reproduce accurately the calculated  $U_{\text{coh}}$  values. In our third improving attempt, we show that the calculated  $U_{\text{coh}}$  values can be fitted extremely accurately to the expression  $U_{\text{coh}} = A + B/\sqrt{N} + C/N$ , where  $A$ ,  $B$  and  $C$  are adjustable parameters. Then going back to the corresponding general expression for  $U_{\text{coh}}$ , we show that it can reproduce very accurately the calculated  $U_{\text{coh}}$  values of other graphene flakes with various shapes.

It is worth noting that our investigation is restricted to graphene flakes consisting of hexagonal rings, which have more than two adjacent hexagonal rings. However, the ideas of the proposed model can be also applied to graphene flakes, which contain hexagonal rings with less than three adjacent hexagonal rings and the validity of the  $U_{\text{coh}}$  expression, which would be derived, would be extended to all kind of graphene flakes. In addition, the ideas of the proposed model could be probably applicable to other two-dimensional (2-D) clusters, like for instance those of graphene allotropes, boron nitride or some chalcogenides, which also form 2-D structures.

## 2. The method

As already mentioned in the Introduction, we calculate the cohesive energy of HGF-ZZ with up to  $\approx 1000$  atoms, using the tight binding molecular dynamics method. HGF-ZZ are hexagonal fractions of the infinite graphene sheet, constructed by adding layers of hexagonal carbon rings around a central hexagon (see Figure 1). It is obvious that those structures can be characterised by the number  $n$  of those layers. For convenience, let us call  $n$ -flake the HGF-ZZ, which is constructed by  $n$  such layers, with the 1-flake being

the single  $C_6$  hexagonal ring. The first  $n$ -flakes are shown in Figure 1. To optimise each  $n$ -flake using the damping molecular dynamics technique, the corresponding fraction of the infinite graphene sheet has been used as a starting geometry.

The tight binding approximation has been described in detail elsewhere [29–31], but we will give a brief description for completeness. In the tight binding approximation, the energy  $U$  of a system is written as  $U = U_{\text{atr}} + U_{\text{rep}} + U_{\text{bond}}$ .

$U_{\text{atr}}$  is the attractive term of the energy, which is written as a sum over all the occupied electronic states of the eigenenergies  $\varepsilon_i$  of the tight binding Hamiltonian  $H$ , i.e.  $U_{\text{atr}} = \sum_i \varepsilon_i n_i^{(\text{occ})}$ , where  $H\Psi_i = \varepsilon_i\Psi_i$  and  $n_i^{(\text{occ})}$  is the occupation number of the  $i$ th eigenstate. The tight binding hamiltonian is expressed in a base of the atomic-like orbitals  $|i, l\rangle$ , where  $i$  denotes atoms and  $l$  atomic-like orbitals of atom  $i$ . The matrix elements  $h_{ij}^{ll'}$  =  $\langle i, l | H | j, l' \rangle$  of the tight binding Hamiltonian, have the form  $h_{ij}^{ll'} = \varepsilon_i \delta_{ij} \delta_{ll'} + (1 - \delta_{ij}) V_{ij}^{ll'}(r_{ij}) \theta(r_{ij} - r_{\text{cut}})$ . In this expression, the on-site matrix elements  $\varepsilon_{ij}$  are constant and they are given by Harrison's scheme [32].  $V_{ij}^{ll'}(r_{ij})$  are the hopping integrals, which are expressed as functions of the Slater–Koster parameters [33]  $V_{ll'm}(r_{ij})$  and the direction cosines.  $\theta(r_{\text{cut}} - r_{ij})$  is the well-known step function, used to restrict the interactions only between first nearest neighbours. The scaling of the Slater–Koster parameters with respect to the interatomic distance is given by [29–31]  $V_{ll'm}(r_{ij}) = V_{ll'm}(d) e^{-\alpha(r_{ij}-d)}$ , where  $V_{ll'm}(d)$  are the Slater–Koster parameters at the bulk interatomic distance  $d$ , as obtained by Harrison's scheme [32].

$U_{\text{rep}}$  is the repulsive term of the energy, which is expressed as  $U_{\text{rep}} = \sum_{i>j} \Phi_0 e^{-\beta(r_{ij}-d)} \theta(r_{\text{cut}} - r_{ij})$ , (i.e. a sum of the pair potentials  $\Phi_0 e^{-\beta(r_{ij}-d)}$  between first nearest neighbours).  $\Phi_0$ ,  $\alpha$  and  $\beta$  are adjustable parameters, which for our case take the values  $\Phi_0 = 4.015576$  eV,  $\alpha = 0.77746 \text{ \AA}^{-1}$  and  $\beta = 4\alpha$ . Those values are determined by fitting the equilibrium bond length  $r_e$  and vibrational frequency  $\omega_e$  of  $C_2$  to their experimental values [34]  $r_e = 1.2378 \text{ \AA}$  and  $\omega_e = 1829.57 \text{ cm}^{-1}$ , respectively.

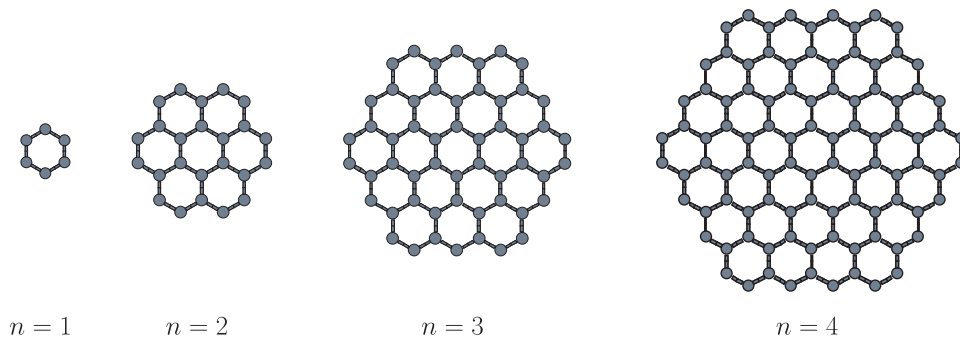


Figure 1. Construction of HGF-ZZ. Each  $n$ -flake is constructed by adding a layer of hexagons around the  $(n - 1)$ -flake.

$U_{\text{bond}}$  is a correction term, firstly introduced by Tománek and Schlüter [35,36], which originally has the form  $U_{\text{bond}} = N(a + b(n_b/N) + c(n_b/N)^2)$ , where  $a$ ,  $b$  and  $c$  are adjustable parameters and  $n_b/N$  is the number of bonds per atom. In our case, we use the form  $U_{\text{bond}} = N(a + b(n_b/N))$  for simplicity. The adjustable parameters  $a$  and  $b$  were determined by fitting the cohesive energy of the equilibrium geometry of  $C_2$  and  $I_h-C_{60}$ , to the values  $U_{\text{coh}}(C_2) = -3.10$  eV (see Ref. [34]) and  $U_{\text{coh}}(C_{60}) = -6.96$  eV (see Ref. [37]), respectively, and they take the values  $a = 17.20$  eV and  $b = 55.55$  eV. The value of  $U_{\text{coh}}(C_{60})$  has been determined from the experimental value of the formation energy for the interaction  $60C(\text{graphene}) \rightarrow C_{60}$ , which is  $23.5 - 26.0$  eV per  $C_{60}$  molecule [37] or  $0.41 \pm 0.02$  eV/atom. Since the cohesive energy of graphene is [38]  $U_{\text{coh}}(\text{graphene}) = -7.37$  eV, the cohesive energy of  $C_{60}$  is  $U_{\text{coh}}(C_{60}) = -7.37 + 0.41 = -6.96$  eV.

The dynamics of the system is governed by the forces  $\mathbf{F}_i = -\nabla_i U_{\text{atr}} - \nabla_i U_{\text{rep}} - \nabla_i U_{\text{bond}}$  acting on each atom- $i$ , where  $\nabla_i U_{\text{bond}} = 0$ ,  $\nabla_i U_{\text{rep}}$  is given by an analytic expression and  $\nabla_i U_{\text{atr}}$  is obtained using the Hellman-Feynman theorem for  $\epsilon_j$ ,  $\nabla_i \epsilon_j = \langle \Psi_j | \nabla_i H | \Psi_j \rangle$ . At each time step of the molecular dynamics procedure, the Newton's equations of motion are solved numerically, using a fifth order Gear's predictor-corrector algorithm [39] and then the velocity of each atom is lowered by 0.1%. The optimum energetically structure of each flake is obtained when all the forces are smaller than a force tolerance value, which in our case is  $10^{-4}$  eV/Å or smaller.

### 3. The model

The model, which is proposed here, is based on the assumption that the binding energy  $U_{\text{bind}}$  of a cluster can be written as a sum of energy contributions from each atom of the cluster, which depend on the local atomic environment of each particular atom of the cluster. In the most general case, the cohesive energy  $U_{\text{coh}}$  of an  $N$ -atom cluster should be written as

$$U_{\text{coh}} = \frac{1}{N} U_{\text{bind}} = \frac{1}{N} \sum_{i=1}^N V_i^{(\text{atom})}, \quad (3)$$

where  $V_i^{(\text{atom})}$  is the above-mentioned energy contribution of atom- $i$  to the binding energy  $U_{\text{bind}}$  of the cluster.

According to the model, the atoms of a cluster with the same local atomic environment contribute the same to the binding energy. Therefore, those atoms can be considered as group and Equation (3) could be written as

$$U_{\text{coh}} = \sum_{i=1}^{n_g} \frac{n_i}{N} V_i, \quad \text{with} \quad \sum_{i=1}^{n_g} n_i = N, \quad (4)$$

where  $n_i$  is the number of the members of group  $i$ ,  $V_i$  is the energy contribution of each atom of that group and  $n_g$  is the number of those different groups. Obviously, the number of the free parameters  $V_i$  of the model is determined by the number  $n_g$  of those different groups. The main task therefore is to properly choose those atom groups, making some reasonable assumptions for the local atomic environment. For instance, if a cluster retains the atomic arrangement of the bulk material far from its boundaries (as it happens with the HGF-ZZ of our study), then the bonding between the atoms far from the boundaries should be more or less the same with that of the bulk material. Therefore the atoms far from the boundaries may be considered as a group having the same local atomic environment. The contribution of this group of atoms to the binding energy will increase as the number of cluster atoms increases and will become dominant for large clusters. If  $V_{\text{bulk}}$  is the contribution of each one of them to the binding energy, then Equation (4) could be written as

$$U_{\text{coh}} = V_{\text{bulk}} + \sum_{i,i \neq \text{bulk}} \frac{n_i}{N} (V_i - V_{\text{bulk}}). \quad (5)$$

Obviously,  $V_{\text{bulk}}$  is the cohesive energy of the bulk material, since for all the other contributions  $n_i/N \rightarrow 0$ , for  $N \rightarrow \infty$ . Let us assume, therefore, that the energy contribution of the 'boundary' atoms is different from that of the 'bulk' atoms and let us use this assumption as a starting point to derive a model for the graphene flake energetics. For simplicity, let us assume that the atoms, which are considered as 'boundary' atoms, are only the twofold coordinated atoms, while the threefold coordinated atoms are considered as 'bulk' atoms.

### 4. Results and discussion

Based on the assumption above, we propose three models of increasing complexity for the graphene flake energetics. In the simplest model, we assume that the contribution of each atom of the flake to the binding energy depends only on the number of  $sp^2$  bonds associated with that atom. Therefore, if  $V_2$  and  $V_3$  are the energy contributions from a twofold and threefold coordinated atom, respectively, then  $V_2 = V_b$  and  $V_3 = 3/2V_b$ , where  $V_b$  is the average bond strength, including an average contribution from the  $p_z$  orbitals. This description is equivalent to the assumption that each bond contributes to the binding energy, an amount of energy equal to  $V_b$  and consequently the energy depends on one parameter only ( $V_b$ , or  $V_3$ , or  $V_2$ ). In the second model, we assume that  $V_3$  and  $V_2$  are independent parameters and therefore  $U_{\text{coh}}$  will depend on two parameters ( $V_3$  and  $V_2$ ). In the third model, we assume that  $V_2$  is different for zig-zag atoms and arm-chair atoms. A zig-zag atom is connected with two threefold coordinated atoms, while an arm-chair atom is connected with one twofold and one

threefold coordinated atom. In the case of our hexagonal flakes, the zig-zag atoms appear at the edges, while the arm-chair atoms appear at the corners. Consequently, the assumption that the local atomic environment of a zig-zag atom is different from that of an arm-chair atom, is reasonable. If  $V_{ac}$  and  $V_{zz}$  are the contributions to the binding energy of each arm-chair (corner) and zig-zag (edge) atom, respectively, then  $U_{coh}$  will depend on three parameters ( $V_3$ ,  $V_{ac}$  and  $V_{zz}$ ). For convenience, let us call those models 'the one-parameter model', 'the two-parameter model' and 'the three-parameter model', respectively.

For the one-parameter model (1-PM)

$$U_{coh} = \frac{n_b}{N} V_b = \frac{2}{3} \frac{n_b}{N} V_3, \quad (6)$$

where  $n_b$  is the total number of bonds of the flake. It is easy to show that each  $n$ -flake can be constructed by adding  $6(2n + 1)$  atoms around the  $(n - 1)$  flake (see Figure 1). Therefore the number  $N$  of the total number of atoms of an  $n$ -flake is

$$N = 6 \sum_{k=1}^n (2k - 1) = 6n^2. \quad (7)$$

Let us denote by  $n_2$  and  $n_3$  the number of the twofold and threefold coordinated atoms of an  $n$ -flake, respectively. It is easy to show that  $n_2 = 6n$ . Using Equation (7), we find  $n_2 = 6n = \sqrt{6N}$  and  $n_3 = N - n_2 = 6n(n - 1) = N - \sqrt{6N}$ . Consequently,  $n_b/N = 3n_3/(2N) + n_2/N = 3/2 - n_2/(2N) = 3/2 - \sqrt{3}/(2N)$  and Equation (6) becomes

$$U_{coh} = \left(1 - \sqrt{\frac{2}{3N}}\right) V_3. \quad (8)$$

For the two-parameter model (2-PM),

$$U_{coh} = \frac{n_3}{N} V_3 + \frac{n_2}{N} V_2 = V_3 + \frac{n_2}{N} (V_2 - V_3). \quad (9)$$

Using the relations between  $n_2$  and  $n_3$  with  $N$  for the HGF-ZZ, Equation (9) becomes

$$U_{coh} = V_3 + \frac{\sqrt{6}(V_2 - V_3)}{\sqrt{N}}. \quad (10)$$

As one can see, this equation has the same functional form with Equation (2) of Kuc *et al.* [11], indicating a linear relation between  $U_{coh}$  and  $N^{-1/2}$ .

For the three-parameter model (3-PM),

$$U_{coh} = \frac{n_3}{N} V_3 + \frac{n_{zz}}{N} V_{zz} + \frac{n_{ac}}{N} V_{ac}, \quad (11)$$

where  $n_{ac}$  and  $n_{zz}$  denote the number of arm-chair and zig-zag atoms of the flake, respectively. It is obvious that

for the HGF-ZZ,  $n_{ac} = 12$  and  $n_{zz} = n_2 - n_{ac}$ , and consequently  $n_{zz} = 6(n - 2) = \sqrt{6N} - 12$ . Thus, for the HGF-ZZ, Equation (11) can be written as

$$U_{coh} = V_3 + \frac{\sqrt{6}(V_{zz} - V_3)}{\sqrt{N}} + \frac{12(V_{ac} - V_{zz})}{N}. \quad (12)$$

According to Equation (8),  $U_{coh}$  of HGF-ZZ is linear on  $1 - \sqrt{2}/(3N)$ , with zero intercept. According to Equation (10),  $U_{coh}$  of HGF-ZZ is linear on  $1/\sqrt{N}$ . According to Equation (12),  $U_{coh}$  of HGF-ZZ has a quadratic dependence on  $1/\sqrt{N}$ . Using the least square fitting method, we can see which model fits better to the  $U_{coh}$  calculated values.

In Figure 2, we present the calculated  $U_{coh}$  values of the HGF-ZZ of our study against  $1 - \sqrt{2}/(3N)$  (Figure 2(a)) and  $1/\sqrt{N}$  (Figure 2(b) and (c)), together with the least square fitting lines predicted by Equations (8), (10) and (12), respectively. The calculated  $U_{coh}$  values are depicted with the black circles. The red dashed lines represent the above least square fitting lines. In the insets of those figures, we show the difference  $\Delta U_{coh}$  between calculated and fitted values for each model. The adjustable parameters of each model, obtained from the fittings are shown in the left part of Table 1. Considering that the energy contribution to the binding energy of each atom of the flake, could be equally partitioned to the bonds of that atom, we can estimate the strength of each bond using the values of  $V_3$ ,  $V_2$ ,  $V_{ac}$  and  $V_{zz}$ . Thus, the strength of the bonds for the one-parameter model is  $V_b = 2V_3/3$ . For the two-parameter model  $V_b^{(3)} = 2V_3/3$  and  $V_b^{(2)} = V_2$ , where  $V_b^{(3)}$  and  $V_b^{(2)}$  are the strengths of the surface and the edge atom bonds, respectively. For the three-parameter model,  $V_{ac-ac} = V_{ac}$ ,  $V_{ac-3} = V_{ac}/2 + V_3/3$ ,  $V_{zz-3} = V_{zz}/2 + V_3/3$  and  $V_{3-3} = 2V_3/3$ , where  $V_{a-b}$  denotes the strength of the bond between  $a$  and  $b$  type of carbon atoms. The values of the strength of the bonds for the three models are shown in the right part of Table 1.

As we can see from the inset of Figure 2(a),  $|\Delta U_{coh}| < 15$  meV, indicating an almost linear dependence of  $U_{coh}$  on  $1 - \sqrt{2}/(3N)$ . However, a more detailed examination of Figure 2(a) shows that the calculated  $U_{coh}$  values exhibit a small curvature against  $1 - \sqrt{2}/(3N)$ , which is also shown from the  $\Delta U_{coh}$  values of the inset. Consequently, the one-parameter model needs improvement.

Since  $U_{coh}$  does not have a linear dependence on  $1 - \sqrt{2}/(3N)$ , it will also not have a linear dependence on  $1/\sqrt{N}$ , because  $N^{-1/2}$  and  $1 - (3N/2)^{-1/2}$  are linearly related. This can be clearly seen in Figure 2(b). Thus, the two-parameter model is also not adequate to describe correctly the graphene flake energetics. However, the small values of  $\Delta U_{coh}$  ( $|\Delta U_{coh}| < 20$  meV) presented in the inset of Figure 2(b), indicate that the relation between  $U_{coh}$  and  $1/\sqrt{N}$  is not far from linear. Moreover, the very small difference between  $V_b^{(3)}$  and  $V_b^{(2)}$  (they differ only by  $\approx 0.015$  eV)

Table 1. Parameters (left part of the table) and bond strength (right part of the table) of the one-, two- and three-parameter models.

Parameters	1-PM	2-PM	3-PM	1-PM	2-PM	3-PM
$V_3$	-7.2804	-7.2834	-7.3143	$V_b = -4.8536$	$V_b^{(3)} = -4.8556$	$V_{3-3} = -4.8762$
$V_2$		-4.8412			$V_b^{(2)} = -4.8412$	$V_{ac-3} = -4.8559$
$V_{zz}$			-4.5754			$V_{zz-3} = -4.7258$
$V_{ac}$			-4.8356			$V_{ac-ac} = -4.8356$

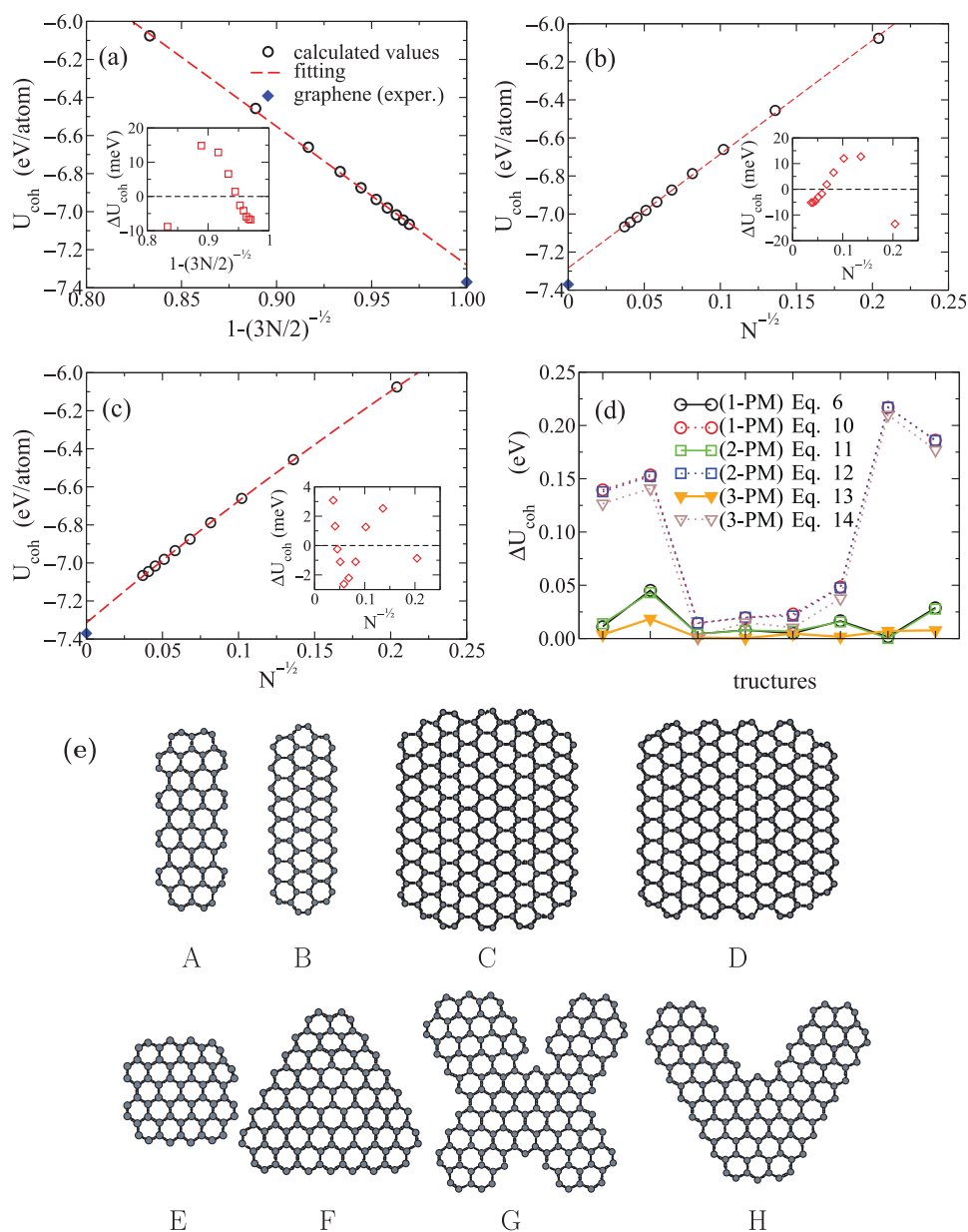


Figure 2. (Color online) (a) Cohesive energy of HGF-ZZ versus  $1 - \sqrt{2/(3N)}$ . The fitting line corresponds to Equation (8) of the 1-PM. (b) Cohesive energy of HGF-ZZ versus  $1/\sqrt{N}$ . The fitting line corresponds to Equation (10) of the 2-PM. (c) Cohesive energy of HGF-ZZ versus  $1/\sqrt{N}$ . The fitting line corresponds to Equation (12) of the 3-PM. (The insets of (a), (b) and (c) show the difference  $\Delta U_{\text{coh}}$  between calculated and fitted values of each model.) (d) The absolute difference  $\Delta U_{\text{coh}}$  between calculated and fitted values for the non-hexagonal flakes, which were used to test the validity of the three models. (e) The structures of the non-hexagonal flakes used to test the validity of the three models.

indicates that the one- and the two-parameter models do not differ dramatically with each other. This can also be seen comparing the deviations  $\Delta U_{\text{coh}}$  of the two models, which are more or less the same.

A quadratic fitting to the calculated  $U_{\text{coh}}$  values versus  $1/\sqrt{N}$  (see Figure 2(c)) shows clearly that Equation (12) of the three-parameter model fits extremely accurately to the calculated  $U_{\text{coh}}$  values. From the inset of Figure 2(c) we can see that  $|\Delta U_{\text{coh}}| < 3$  meV, which is five times smaller than the corresponding value (0.015 eV) for the one- and two-parameter models. Moreover,  $V_{3-3} < V_{\text{ac}-3} < V_{\text{ac-ac}} < V_{\text{zz}-3}$ . The (3-3), (ac-3) and (ac-ac) bonds seems to have almost the same strength, differing with each other by  $\approx 0.02$  eV. The (zz-3) bond seems to be the weakest, with  $\approx 0.11$  eV bond-strength difference from the (ac-ac) bond. This difference is considerably higher than the corresponding difference between  $V_b^{(3)}$  and  $V_b^{(2)}$  of the two-parameter model, which is only 0.015 eV. However, any comparison between bond strengths needs further investigation, because their differences seem to be very small and they might be affected by the fitting.

To test the validity of Equation (11), we calculate the cohesive energy of several non-hexagonal graphene flakes using the tight binding molecular dynamics method and we compare the calculated cohesive energy values with the values obtained by Equation (11). We also compare the calculated  $U_{\text{coh}}$  values of those non-hexagonal flakes with the predictions of Equations (6), (8)–(10) and (12), which has been derived from the one-, two- and three-parameter models. The graphene flakes we use for the validity test, are shown in Figure 2(e) and they include elongated structures along the arm-chair and the zig-zag edges (structures A and B, respectively), square-like structures (C, D and E), a triangular structure (F) and complicated shape flakes (G and H), constituting a representative set of random graphene flakes. In Figure 2(d) we show the absolute value of  $\Delta U_{\text{coh}}$  for Equations (6), (8)–(12). As one can see, the smallest error corresponds to the general equation of the three-parameter model (Equation (11)), which indicates that Equation (11) is valid not only for HGF-ZZ, but also for graphene flakes with random shape.

As expected, the errors corresponding to the general equations of the three models (Equations (6), (9) and (11)) are always smaller than the errors corresponding to the equations for HGF-ZZ (Equations (8), (10) and (12)) and the errors corresponding to the one- and two-parameter models are almost the same with each other, either for the general expressions (Equations (6) and (9)), or for the expressions corresponding to HGF-ZZ (Equations (8) and (10)).

Among the errors of the expressions of the three models for HGF-ZZ (Equations (8), (10) and (12)), the error of Equation (12), corresponding to the three-parameter model is smaller. Moreover, the prediction error of those three equations is smaller for the cyclic structures C, D and E

than the others structures, approaching the error of the general expressions. As the shape deviates from cyclic, the error increases, following the sequence: triangle (structure F), elongated structures (A and B) and complicated shape structures (G and H).

The maximum error for the general expressions of the three models appears for structure B, which is a narrow elongated structure. Its value is much higher compared to the corresponding maximum error, which appears in the inset of Figure 2(c). This indicates that Equation (11) might possibly be further improved so that the prediction error for any graphene flake would become comparable to the values presented in the inset of Figure 2(c). However, using HGF-ZZ for the determination of our model, Equation (11) cannot be further improved.

Let us assume that except of the three local atomic environments we have assumed that they affect the cohesive energy in the three-parameter model, there is another one, which also affects the cohesive energy. Under these conditions and according to Equation (4), the cohesive energy should be written as  $U_{\text{coh}} = \sum_{i=1}^4 V_i n_i / N$ , depending on the four adjustable parameters  $V_i$ . For HGF-ZZ,  $n_i = a_i' n^2 + b_i' n + c_i$ ,  $i = 1, 2, 3, 4$  or (using Equation (7))  $n_i = a_i N + b_i \sqrt{N} + c_i$ , with  $a_i'$ ,  $b_i'$ ,  $a_i$ ,  $b_i$  and  $c_i$  being constants. With those expressions for  $n_i$ ,  $U_{\text{coh}}$  will be written again as  $U_{\text{coh}} = A + B/\sqrt{N} + C/N$ , which means that the number of the independent adjustable parameters of the model is reduced to three, exactly as it happens in the three-parameter model. Therefore, if only HGF-ZZ are used for the fitting, the number of independent  $V_i$  parameters are only three. Consequently, any assumption of more than three local atomic environments is useless. On the other hand, if for the determination of the parameters  $V_i$ , other graphene flakes were involved (so that  $n_i$  were not given from the same expression  $n_i = a_i N + b_i \sqrt{N} + c_i$  for all the flakes), then the number of the adjustable parameters of the model would not be reduced to three and an improvement of Equation (11) might be possible.

Based on the results presented in our study, we can now understand why Kuc *et al.* [11] observed a linear relation between  $U_{\text{coh}}$  and  $N_s/N$ , but not between  $U_{\text{coh}}$  and  $1/\sqrt{N}$ . Obviously, the observed linear relation between  $U_{\text{coh}}$  and  $N_s/N$  is exactly the general prediction of the two-parameter model (see Equation (9)), which (as we have already shown) is just a good approximation of the more accurate Equation (11) of the three-parameter model. Therefore, for the random shape graphene flakes of Kuc *et al.*, the observed linear relation between  $U_{\text{coh}}$  and  $N_s/N$  is reasonable. On the other hand, a possible linear relation between  $U_{\text{coh}}$  and  $1/\sqrt{N}$  can be derived from Equation (9), if and only if  $N_s (= n_2) \propto \sqrt{N}$ . This proportionality is approximately correct for cyclic flakes (like the structures C, D and E of Figure 2(e)) because for cyclic flakes the edge-to-surface ratio is proportional (or almost proportional) to  $\sqrt{N}$ . However, for not cyclic flakes, the edge-to-surface ratio is not

proportional to  $\sqrt{N}$ , not even approximately, and consequently, for those structures the relation between  $U_{\text{coh}}$  and  $1/\sqrt{N}$  is far from linear.

The cohesive energy of cyclic graphene flakes can be also expressed as a function of their diameter  $d$ . The diameter  $d$  of a cyclic flake is proportional to  $\sqrt{N}$ . Consequently, Equation (12) could be written as  $U_{\text{coh}} = A + B'/d + C'/d^2$ , where  $A$ ,  $B'$  and  $C'$  are adjustable constants. This equation seems to agree with the Nakajima and Shintani [10] plots, which show the  $U_{\text{coh}}$  values of families of cyclic graphene flakes as a function of their diameter  $d$ . Nakajima and Shintani use some fitting curves to fit those points; however, they do not report anything about the form of those fitting curves.

It is worth noting that Equation (12) represents the 2-D expression of the liquid drop model [40–51]. According to the liquid drop model for the three-dimensional (3-D) clusters, the cohesive energy is given by  $U_{\text{coh}} = A_b + A_f N^{-1/3} + A_e N^{-2/3} + A_c N^{-1}$ , where  $A_b, A_f, A_e$  and  $A_c$  are constants. In the above equation,  $A_b$  represents the bulk cohesive energy and the rest of the terms represent corrections to  $A_b$  due to the surface effects. Thus, the second term represents the facet atoms correction and is proportional to the surface-to-bulk ratio  $N^{-1/3}$ . The third term represents the edge atoms correction and is proportional to the edge-to-bulk ratio  $N^{-2/3}$ . The fourth term represents the vertex atoms correction and is proportional to the vertex-to-bulk ratio  $N^{-1}$ . In a 2-D cluster, the analogue of the bulk, face and edge atoms are the surface, edge and corner atoms, respectively. Obviously, there is not any 2-D analogue of the 3-D cluster vertex atoms and consequently, the 2-D analogue of the above equation will contain only three terms. The first term will be a constant term representing the surface atoms contribution, the second term will be proportional to  $1/\sqrt{N}$  (edge-to-surface ratio), representing the edge atom correction and the third term will be proportional to  $1/N$  (corner-to-surface ratio), representing the corner atoms correction. The combination of those three terms leads to Equation (12) and consequently Equation (12) is the 2-D analogue of the above equation.

Based on the present work, two basic rules for the stability of the graphene flakes can be derived. According to the first rule, *between isomers the most stable are those with the larger number of bonds (or equivalently with the smaller number of edge atoms)*. As we have seen, the strength of the graphene flake bonds is almost the same for all the bonds of the flake. The contribution of each bond to the binding energy is  $\approx 4.73 - 4.88$  eV. Thus, the binding energy of a graphene flake is approximately proportional to the number of its bonds. Consequently, between two isomers the more stable is the one with the larger number of bonds. Since  $n_b/N = 3/2 - n_2/2N$ , isomers with the same number of bonds  $n_b$ , have the same number of edge atoms  $n_2$ . Consequently, between two isomers the more stable is the one with the smaller number of edge atoms (i.e. twofold

coordinated atoms). According to the second rule, *between isomers with the same number of bonds (or equivalently with the same number of edge atoms), the most stable are those with the smaller number of zig-zag atoms*. Bearing in mind that  $V_{\text{zz}} > V_{\text{ac}}$ , the second rule is directly derived from the first rule. The edge atoms would be either zig-zag or arm-chair atoms and consequently between two isomers with the same number of edge atoms the cohesive energy will be smaller for the isomer with less zig-zag atoms. Those two rules can be used for a raw estimation of the stability of graphene flakes, before an accurate prediction using Equation (11).

## 5. Conclusion

In the present work, we propose a model for the energetics of graphene flakes, which is based on the idea that the binding energy of a cluster is a sum of atomic energy contributions, which depend on the local atomic environment of each atom of the cluster. We showed that the proposed model can reproduce very accurately the cohesive energy of graphene flakes calculated using the tight binding molecular dynamics method.

We first calculated the cohesive energy values of HGF-ZZ with up to  $\approx 1000$  atoms, which we fit to the cohesive energy expressions proposed by the model in order to determine their adjustable parameters. We presented three such expressions with increasing level of accuracy and their counterparts for HGF-ZZ, which are derived from the general expression. Equation (11), which is the expressions with the highest level of accuracy, fits extremely accurately to the HGF-ZZ cohesive energy values and can reproduce very accurately the cohesive energy of other graphene flakes with various shapes. Equation (11) has been derived considering different local atomic environments between the threefold coordinated atoms, the zig-zag atoms and the arm-chair atoms. We further showed that Equation (12) (the counterpart of Equation (11) for HGF-ZZ) can be considered as the 2-D analogue of the liquid drop model.

We also showed that the stability of graphene flakes obeys the following rules: (1) between isomers the most stable are those with the larger number of bonds (or equivalently with the smaller number of edge atoms) and (2) between isomers with the same number of bonds (or equivalently with the same number of edge atoms), the most stable are those with the smaller number of zig-zag atoms.

Our study is restricted to graphene flakes with hexagonal rings having more than two adjacent hexagonal rings, but the proposed model can be easily generalised to cover all the graphene flakes.

## Acknowledgements

The author would like to thank Prof Madhu Menon for providing the tight binding molecular dynamics code and Prof David

Tománek for valuable discussions. Computational resources have been provided by the computer center of the Institute of Electronic Structure and Laser - FORTH, Greece.

## References

- [1] A.K. Geim and K.S. Novoselov, *Nat. Mater.* **6**, 183 (2007).
- [2] A.A. Green and M.C. Hersam, *Nano Lett.* **9**, 4031 (2009).
- [3] D. Geng, B. Wu, Y. Guo, L. Huang, Y. Xue, J. Chen, G. Yu, L. Jiang, W. Hu, and Y. Liu, *Proc. Nat. Acad. Sci.* **109**, 7992 (2012).
- [4] L. Ci, L. Song, D. Jariwala, A.L. Elias, W. Gao, M. Terrones, and P.M. Ajayan, *Adv. Mater.* **21**, 4487 (2009).
- [5] Z. Luo, S. Kim, N. Kawamoto, A.M. Rappe, and A.T.C. Johnson, *ACS Nano* **5**, 9154 (2011).
- [6] J. Kwon, S.H. Lee, K.H. Park, D.H. Seo, J. Lee, B.S. Kong, K. Kang, and S. Jeon, *Small* **7**, 864 (2011).
- [7] K.S. Subrahmanyam, L.S. Panchakarla, A. Govindaraj, and C.N.R. Rao, *J. Phys. Chem. C* **113**, 4257 (2009).
- [8] T. Moldt, A. Eckmann, P. Klar, S.V. Morozov, A.A. Zhukov, K.S. Novoselov, and C. Casiraghi, *ACS Nano* **5**, 7700 (2011).
- [9] A.S. Barnard and I.K. Snook, *Model. Simul. Mater. Sci. Eng.* **19**, 054001 (2011).
- [10] T. Nakajima and K. Shintani, *J. Appl. Phys.* **106**, 114305 (2009).
- [11] A. Kuc, T. Heine, and G. Seifert, *Phys. Rev. B* **81**, 085430 (2010).
- [12] F. Molitor, J. Gttinger, C. Stampfer, S. Drscher, A. Jacobsen, T. Ihn, and K. Ensslin, *J. Phys.: Condens. Matter* **23**, 243201 (2011).
- [13] A.M. Silva, M.S. Pires, V.N. Freire, E.L. Albuquerque, D.L. Azevedo, and E.W.S. Caetano, *J. Phys. Chem. C* **114**, 17472 (2010).
- [14] A.K. Singh, E.S. Penev, and B.I. Yakobson, *Comput. Phys. Commun.* **182**, 804 (2011).
- [15] H. Tachikawa and H. Kawabata, *J. Phys. B: At. Mol. Opt. Phys.* **44**, 205105 (2011).
- [16] C.D. Reddy, S. Rajendran, and K.M. Liew, *Nanotechnology* **17**, 864 (2006).
- [17] P.S. Branicio, M.H. Jhon, C.K. Gan, and D.J. Srolovitz, *Model. Simul. Mater. Sci. Eng.* **19**, 054002 (2011).
- [18] B. Huang, M. Liu, N. Su, J. Wu, W. Duan, B.I. Gu, and F. Liu, *Phys. Rev. Lett.* **102**, 166404 (2009).
- [19] H.P. Heiskanen, M. Manninen, and J. Akola, *New J. Phys.* **10**, 103015 (2008).
- [20] D.A. Bahamon, A.L.C. Pereira, and P.A. Schulz, *Phys. Rev. B* **79**, 125414 (2009).
- [21] V.B. Shenoy, C.D. Reddy, A. Ramasubramaniam, and Y.W. Zhang, *Phys. Rev. Lett.* **101**, 245501 (2008).
- [22] I. Romanovsky, C. Yannouleas, and U. Landman, *Phys. Rev. B* **79**, 075311 (2009).
- [23] I. Romanovsky, C. Yannouleas, and U. Landman, *Phys. Rev. B* **85**, 165434 (2012).
- [24] P. Potasz, A.D. Güçlü, A. Wójs, and P. Hawrylak, *Phys. Rev. B* **85**, 075431 (2012).
- [25] Y. Zhou, Z. Wang, P. Yang, X. Sun, X. Zu, and F. Gao, *J. Phys. Chem. C* **116** (9), 5531 (2012).
- [26] X.W. Sha, E.N. Economou, D.A. Papaconstantopoulos, M. Pederson, M.J. Mehl, and M. Kafesaki, in *APS Meeting Abstracts*, p. 11014 (Boston, MA, 2012).
- [27] C.O. Girit, J.C. Meyer, R. Erni, M.D. Rossell, C. Kisielowski, L. Yang, C.H. Park, M.F. Crommie, M.L. Cohen, S.G. Louie, and A. Zettl, *Science* **323**, 1705 (2009).
- [28] D. Tománek, S. Mukherjee, and K.H. Bennemann, *Phys. Rev. B* **28**, 665 (1983).
- [29] A.N. Andriotis, M. Menon, G.E. Froudakis, Z. Fthenakis, and J. Lowther, *Chem. Phys. Lett.* **292**, 487 (1998).
- [30] M. Menon, J. Connolly, N. Lathiotakis, and A. Andriotis, *Phys. Rev. B* **50**, 8903 (1994).
- [31] N.N. Lathiotakis, A.N. Andriotis, M. Menon, and J. Connolly, *J. Chem. Phys.* **104**, 992 (1996).
- [32] W.A. Harrison, *Electronic Structure and the Properties of Solids* (Dover, New York, 1989).
- [33] J.C. Slater and G.F. Koster, *Phys. Rev.* **94**, 1498 (1954).
- [34] K.P. Huber and G. Herzberg, *Molecular Spectra and Molecular Structure IV, Constants of Diatomic Molecules* (Van Nostrand Reinhold, New York, 1979).
- [35] D. Tománek and M.A. Schlüter, *Phys. Rev. B* **36**, 1208 (1987).
- [36] D. Tománek and M.A. Schlüter, *Phys. Rev. Lett.* **56**, 1055 (1986).
- [37] H.S. Chen, A.R. Kortan, R.C. Haddon, M.L. Kaplan, C.H. Chen, A.M. Mujsce, H. Chou, and D.A. Fleming, *Appl. Phys. Lett.* **59**, 2956 (1991).
- [38] C. Kittel, *Introduction to Solid State Physics* (John Wiley and Sons, New York, 2005).
- [39] C.W. Gear, Technical Report 7126, Argonne National Laboratory, 1966.
- [40] F. Baletto and R. Ferrando, *Rev. Mod. Phys.* **77**, 371 (2005).
- [41] J.E. Hearn and R.L. Johnston, *J. Chem. Phys.* **107** (12), 4674 (1997).
- [42] J.W. Lee and G.D. Stein, *J. Phys. Chem.* **91**, 2450 (1987).
- [43] J. Xie, J.A. Northby, D.L. Freeman, and J.D. Doll, *J. Chem. Phys.* **91**, 612 (1989).
- [44] J.P. Perdew, P. Ziesche, and C. Fiolhais, *Phys. Rev. B* **47**, 16460 (1993).
- [45] J.P. Perdew, Y. Wang, and E. Engel, *Phys. Rev. Lett.* **66**, 508 (1991).
- [46] J. Jortner, *Z. Phys. D* **24**, 247 (1992).
- [47] J. Uppenbrink and D.J. Wales, *J. Chem. Phys.* **96** (11), 8520 (1992).
- [48] M. Seidl and M. Brack, *Ann. Phys.* **245** (2), 275 (1996).
- [49] D.N. Poenaru, R.A. Gherghescu, A.V. Solov'yov, and W. Greiner, *Europhys. Lett.* **79**, 63001 (2007).
- [50] C. Fiolhais and J.P. Perdew, *Phys. Rev. B* **45**, 6207 (1992).
- [51] M. Brajczewska, C. Fiolhais, and J.P. Perdew, *Int. J. Quantum Chem.* **48**, 249 (1993).